

Article

Thermal Conductivity Calculations for Nanoparticles Embedded in a Base Fluid

Soran M. Mamand

Physics Department, College of Science, University of Sulaimani, Sulaimani 5033, Kurdistan Regional Government, Iraq; soran.mamand@univsul.edu.iq

Abstract: The Prasher analytical model was used for calculating the thermal conductivity of the embedded nanoparticles of Al_2O_3 , CuO , ZnO , and SiO_2 in conventional fluids, such as water and ethylene glycol. The values that were obtained were used in the nanofluid theoretical models for comparison with experimental data, where good agreement was obtained. Liang and Li's theoretical model was also used to calculate the thermal conductivity of these nanoparticles, where the results agreed with those obtained using the Prasher model. The effect of the liquid nanolayer thickness around the nanoparticles that was used to enhance the effective thermal conductivity of nanofluids was explained. The role of the nanoparticles' surface specular parameter, which was size-dependent, was clarified. This theoretical trend provides a simple method for estimating the thermal conductivity of nanoparticles and nanofluids.

Keywords: nanofluid; nanoparticles; thermal conductivity; heat transfer



Citation: Mamand, S.M. Thermal Conductivity Calculations for Nanoparticles Embedded in a Base Fluid. *Appl. Sci.* **2021**, *11*, 1459. <https://doi.org/10.3390/app11041459>

Academic Editor: Guan Heng Yeoh
Received: 3 December 2020
Accepted: 1 February 2021
Published: 5 February 2021

Publisher's Note: MDPI stays neutral with regard to jurisdictional claims in published maps and institutional affiliations.



Copyright: © 2021 by the author. Licensee MDPI, Basel, Switzerland. This article is an open access article distributed under the terms and conditions of the Creative Commons Attribution (CC BY) license (<https://creativecommons.org/licenses/by/4.0/>).

1. Introduction

Traditional thermal fluids, such as ethylene glycol (EG), oil and water, play an important role in many engineering sectors, such as power generation and heating and cooling processes. However, their heat transfer capability is limited by their very low thermal conductivity. Nanofluids (NFs) are fluids produced by the dispersion of metallic or nonmetallic nanoparticles or nanofibers in a liquid. The addition of these dispersed particles in traditional fluids produces an enhancement of the thermal conductivity in the host liquids [1–3]. According to their potential applications in the heat transfer field, NFs have been a subject of intensive investigations [4–9]. Over the past two decades, a significant amount of experimental data has been gathered on the thermal conductivity enhancement capabilities of metallic and oxide nanoparticles, carbon nanofibers, and carbon nanotubes in these traditional fluids. Comprehensive recent reviews and studies about thermal conductivity enhancement and heat transfer characteristics of NFs were presented in the literature [10–19]. Many parameters affected the thermal conductivity of the resultant NFs: the kind of nanoparticles, shape and diameter of the particles, particle volume concentrations, temperatures, type of the base fluid, acidity (pH) of the base fluid, preparation techniques, and clustering [2,6,20]. Several theoretical models and mechanisms have been proposed in the literature for explaining the measured thermal conductivity of NFs using various assumptions [11,21–30]. However, reported works on theoretical and experimental investigations to understand the science and mechanisms behind the thermal conductivity enhancement of NFs continue to be controversial and far from comprehensive [31,32]. Jang and Choi [23,33] concluded that the hydrodynamic effect of the Brownian motion of nanoparticles causes an enhancement in the thermal conductivity of the NFs and was a crucial factor regarding the mechanism governing the thermal behaviors. Contradicting this, Evans et al. [34] suggested that the nanoparticles' Brownian motion had a negligible effect on the extraordinary thermal transport properties of NFs. Evans and co-workers concluded that the nanofluids' thermal conductivity was described by effective medium theory, where aggregation of the particles causes an enhancement of

the nanofluids’ thermal conductivity. Furthermore, experimental studies showed that the nanofluids’ thermal conductivity increased with the decrease of the particle size [35–39], while other studies reported the opposite conclusions, where the thermal conductivity increased with the increase of particle size [40–46].

Recently, Pryazhnikov et al. [47] and Ceotto and Rudyak [48] studied the dependence of NFs’ thermal conductivity on the nanoparticles’ material. They argued and showed that the thermal conductivity of NFs has a direct connection with the density of the nanoparticles’ material, even though they did not focus their attention on the value of the nanoparticles’ thermal conductivity.

Most of the theoretical models for thermal conductivity of NFs embedded with nanoparticles fail to fit the experimental data, maybe because of the lack of nanoparticle thermal conductivity data [49–53]. Practically, however, measuring thermal conductivity for individual nanoparticles is very difficult. Therefore, the objective of this work was to calculate the thermal conductivity of nanoparticles dispersed in EG and water by using the Prasher analytical model [54]. Afterward, the analytical formula that was given by Liang and Li [55] and the Yu and Choi model [56] were used to verify the obtained values of nanoparticles’ thermal conductivity.

2. Theories

Prasher [54] derived an equation based on the solution of the Boltzmann transport equation for calculating the thermal conductivity of nanocomposites made from micro- and nanowires. The effective thermal conductivity of the base-fluid embedded nanowires, K_{ceff} , is given by:

$$K_{ceff} = (1 - \varphi)K_m + \varphi K_w - (\Delta K1 + \Delta K2), \tag{1}$$

where; K_m and K_w are the thermal conductivities of the host medium and nanowire, respectively; φ is the volume fraction of a nanowire;

$$\Delta K1 = \left(\frac{6K_m}{\pi r_2^2} \right) \times \left[\begin{aligned} & \left(\int_{r=r_1}^{r=r_2} \int_{\theta=0}^{\theta=\frac{\pi}{2}} \int_0^{\varnothing_{max}} \exp\left(\frac{-B1}{l_m}\right) r dr \cos^2 \theta \sin \theta d\theta d\varnothing \right) \\ & + \left(\int_{r=r_1}^{r=r_2} \int_{\theta=0}^{\theta=\frac{\pi}{2}} \int_{\pi-\varnothing_{max}}^{\varnothing_{max}} \exp\left(\frac{B2}{l_m}\right) r dr \cos^2 \theta \sin \theta d\theta d\varnothing \right) \end{aligned} \right]; \tag{2}$$

$$\Delta K2 = \left(\frac{6K_w}{\pi r_2^2} \right) \times \left[\int_{r=0}^{r=r_1} \int_{\theta=0}^{\theta=\frac{\pi}{2}} \int_0^{\pi} \exp\left(\frac{-B3}{l_w}\right) r dr \cos^2 \theta \sin \theta d\theta d\varnothing \right]; \tag{3}$$

$B1 = \frac{r \cos \varnothing - \sqrt{(r_1^2 - r^2 \sin^2 \varnothing)}}{\sin \theta}$; $B2 = \frac{\sqrt{(r_1^2 - r^2 \sin^2 \varnothing)} - r \cos \varnothing - 2\sqrt{(r_2^2 - r^2 \sin^2 \varnothing)}}{\sin \theta}$; $B3 = \frac{r \cos \varnothing + \sqrt{(r_1^2 - r^2 \sin^2 \varnothing)}}{\sin \theta}$; r_1 is the radius of the nanowire; r_2 is the radius of the specular phonon scattering at the boundary of the nanowire. Equation (1) is applicable for a grey medium, that is, the mean free path (in the nanowire, l_w , and in the base fluid, l_m) and the phonon velocity does not depend on the phonon frequency [54]. The details of the derivation of Equation (1) and all the parameters in Equations (2) and (3) can be found in [54]. Equation (1) was used in the present work for nanoparticles instead of nanowires dispersed in a given base fluid.

Liang and Li [55] derived a theory for the size-dependent thermal conductivity of nanoscale semiconducting thin films, nanowires, and nanoparticles, in which the mean free path, l , the size effect, L , and the surface scattering effect (through the specularity parameter, β) of phonon transport were considered. The thermal conductivity of a nanomaterial, K , is [55]:

$$K = K_B \beta \exp\left(-\frac{l_0}{L}\right) \cdot \left[\exp\left(\frac{1 - \alpha}{\frac{L}{l_0} - 1}\right) \right]^{3/2} \tag{4}$$

where K_B is the bulk thermal conductivity of the nanoparticles. Definitions of all the parameters can be found in [55]. This theory has been applied to different crystalline nanomaterials [55,57–59].

An experimental study [60] proved that there is an adsorbed layer of liquid molecules around the nanomaterials in NFs. Yu and Choi [56] utilized the Maxwell equation [61] for

the effective thermal conductivity of NFs, which suggested that liquid layering is one of the parameters that are responsible for the enhanced thermal conductivity of NFs. Yu and Choi [56] assumed that an equivalent particle could be formed from the combination with its coated nanolayer with a radius of $r_1 + h$ (where r_1 is the original particle radius and h is the nanolayer thickness). Unfortunately, there is no experimental data for the thermal conductivity of liquid layering. This is why the thermal conductivity of the nanoparticle, K_p , is equal to that of nanolayer, as suggested by Yu and Choi [56]. The conventional Maxwell equation for homogeneous mixtures is [61]:

$$\frac{K_{ceff}}{K_m} = \frac{K_p + 2K_m - 2\varphi(K_m - K_p)}{K_p + 2K_m + \varphi(K_m - K_p)}. \quad (5)$$

This Maxwell equation can be modified to [56]:

$$\frac{K_{ceff}}{K_m} = \frac{[K_p + 2K_m + 2\varphi(K_p - K_m)(1 + \lambda)^3]}{[K_p + 2K_m - \varphi(K_p - K_m)(1 + \lambda)^3]}, \quad (6)$$

where λ is equal to h/r_1 .

3. Results

According to the experimental data obtained at room temperature by Eastman et al. [62], calculations of the thermal conductivity ratio (the ratio between the effective thermal conductivity of the NFs and the thermal conductivity of the base fluid) for copper oxide (CuO) and alumina (Al₂O₃) nanoparticles of diameters 36 nm and 33 nm, respectively, that were dispersed in deionized water were performed using Equation (1). The results are delineated (dotted lines) in Figure 1. The thermal conductivities of CuO and Al₂O₃ nanoparticles found using the trial and error method were equal to 7.8 W/m·K and 4 W/m·K, respectively. According to Yu and Choi's model (Equation (6)), these results (7.8 W/m·K and 4 W/m·K) give a good thermal conductivity ratio compared to that of the experimental data shown in Figure 1. The data of the base fluid, nanoparticles, and the parameter values are shown in Table 1. However, the thermal conductivities of the two oxide nanoparticles were calculated based on Equation (4) and Tables 1 and 2, which give 7.76 W/m·K and 4.04 W/m·K, respectively, and were in good agreement with the results obtained using Equation (1).

In Figure 1, for comparative purposes, Kole and Dey's [63] calculations were considered for the Al₂O₃ nanoparticles represented by Eastman et al.'s [62] data. Kole and Dey [63] used Feng et al.'s [64] model, in which contributions from both the interfacial layer and aggregation of the nanoparticles were taken into account. The results underpredicted the reported data. Kole and Dey [63] attributed this underprediction of their calculations to another contributing parameter that may be required to predict the thermal conductivity ratio of NFs. A detailed exposition that discusses the results and parameters is provided in the next section.

The same calculation procedure was performed for 20 nm ZnO nanoparticles that were dispersed in EG with Yu et al.'s [52] experimental data by using Equations (1) and (6) and Table 1. The results are reported in Figure 2. The obtained thermal conductivity value 1.6 W/m·K of ZnO nanoparticles obtained from Equation (1) was close to that of the previously reported values of 1.4 W/m·K for polycrystalline ZnO thin films [65], and 1.16 W/m·K for 20 nm ZnO nanoparticles [66]. However, according to the theoretical model of Chen et al. [67], calculations of the thermal conductivity ratio due to aggregations of nanoparticles were performed by Yu et al. [52] for their experimental data (solid blue-line), as seen in Figure 2. Our calculation was more precise than Yu et al.'s [52] calculation.

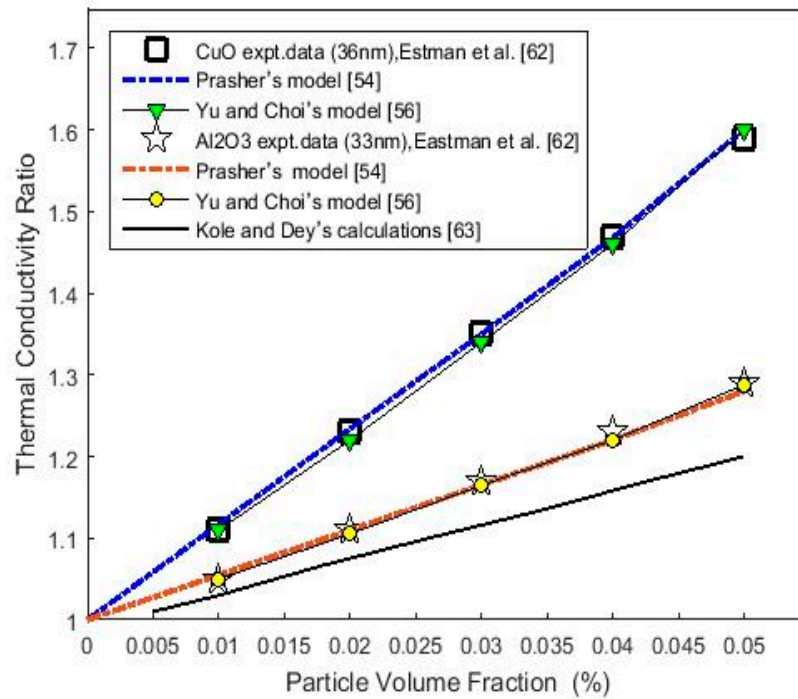


Figure 1. (Color online) Calculated thermal conductivity ratio (K_{ceff}/K_m) versus the particle volume fraction for Al_2O_3 and CuO nanoparticles in a water base fluid using the Prasher’s model (Equation (1)) and Yu and Choi’s model (Equation (6)). Expt. data are from [62]. The solid black-line is from Kole and Dey’s calculations [63].

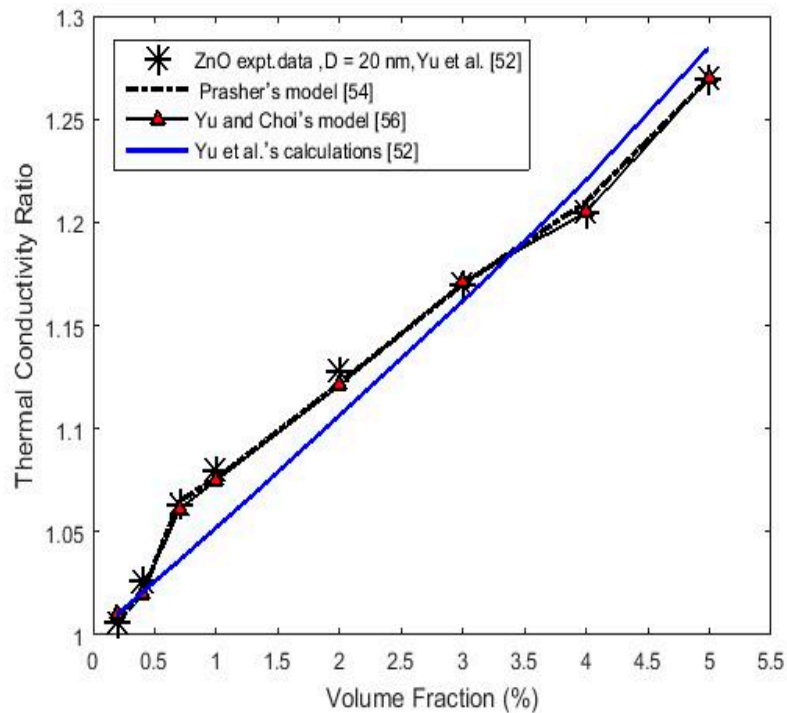


Figure 2. (Color online) Calculated thermal conductivity ratio (K_{ceff}/K_m) versus the nanoparticle volume fraction for a ZnO –ethylene glycol (EG) nanofluid, using the Prasher’s (Equation (1)) and Yu and Choi’s models (Equation (6)). Experimental data are from [52]. The solid blue-line represents Yu et al.’s calculations [52].

Using Equation (4) and the data in Tables 1 and 2, a calculation of the thermal conductivity of ZnO nanoparticles with a phonon mean free path, l , equal to 24.35 nm as estimated by the equation $l = 10aT_m/\gamma T$ [68], where a is the lattice constant equal to 0.325 nm [69], $\gamma \approx 1$ is the Gruneisen parameter [33], T is the absolute temperature equal to 300 K, and T_m is the melting point—gives the value of 1.618 W/m·K, which agrees well with the value obtained by using Equation (1).

Table 1. The nanoparticle and base fluid data at $T = 300$ K.

Parameters	Water	EG	ZnO	SiO ₂	Al ₂ O ₃	CuO
Bulk conductivity (W/m·K)	0.61 ^a	0.25 ^a	37 ^c	2–4 ^d	30 ^f	32.9 ^f
Mean free path (nm)	0.738 ^a	0.875 ^a	24.35 ^g	0.6 ^e	35 ^a	27 ^a
Nanoparticle conductivity(W/m·K) ^b			1.61	1.39	4	7.8
h in Equation (6) ^b			3–2.8	2.9–1.5	6.4–6	11–10.8

^a: [33], ^b: present work, ^c: (for wurtzite ZnO) [66], ^d: [70], ^e: [71], ^f: [72], ^g: calculated using the equation in [68].

Furthermore, for the sake of verifying this trend, the same calculation method was used for SiO₂ nanoparticles that were 20 nm in diameter and dispersed in water, where the results are plotted versus the particle volume concentration for the experimental data reported by Kang et al. [70] in Figure 3. The value of 1.39 W/m·K for thermal conductivity that was obtained using Equation (1) agrees well with that of the experimental data and is equal to that obtained by using Equation (4) and the data in Tables 1 and 2, which was 1.391 W/m·K.

Table 2. Material properties of oxide nanoparticles (at $T = 300$ K) used in Equation (4).

Parameters	ZnO	SiO ₂	Al ₂ O ₃	CuO
Melting temperature (K)	2248 ^b	1700 ^d	2345 ^f	1600 ⁱ
Formation enthalpy (kJ/mol)	350 ^b	9.39 ^d	167.5 ^g	156.06 ^j
Interatomic distance (nm)	0.1976 ^c	0.16 ^e	0.176 ^h	0.172 ^k
Specularity parameter β	0.45 ^a	0.46 ^a	0.55 ^a	0.69 ^a

^a: present work, ^b: [73], ^c: [74], ^d: [75], ^e: [76], ^f: [77], ^g: [78], ^h: [79], ⁱ: [80], ^j: [81], ^k: [82].

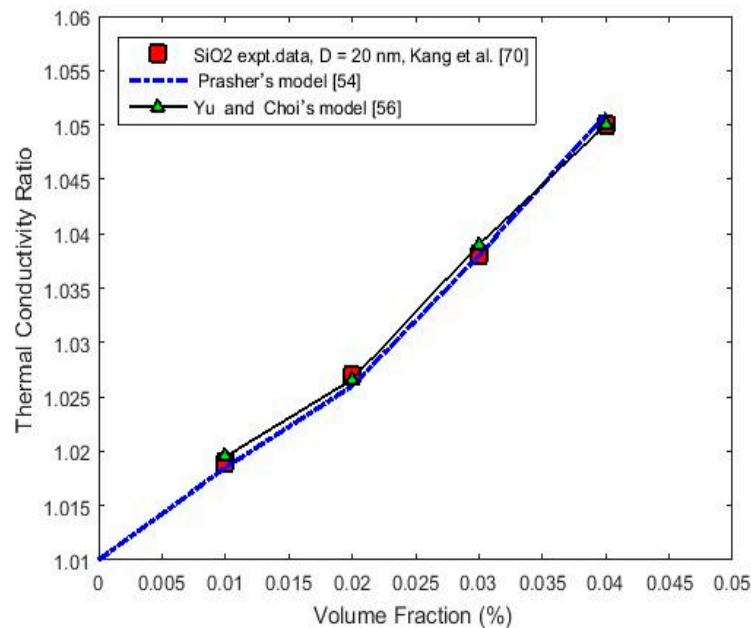


Figure 3. (Color online) Calculated thermal conductivity ratio (K_{ceff}/K_m) versus the nanoparticle volume fraction for a SiO₂–water NF using Prasher’s (Equation (1)) and Yu and Choi’s (Equation (6)) models. Experimental data are from [70].

4. Discussion

4.1. Nanoparticles' Thermal Conductivity and Specularity Parameter, β

Experimental investigations [47,48,83,84] and the molecular dynamics method [85,86] revealed that an increase in the thermal conductivity of nanofluids is related to an increase in the nanoparticle material density rather than its material. The density of a nanosized material is a size-dependent parameter. Abdullah et al. [87] showed that the densities of Si nanoparticles with 20 nm and 5 nm diameters decrease by amounts of 6% and 18%, respectively. Experimental studies [88,89] have also shown that the density of nanosized materials decreases as their size decreases, particularly at a diameter of less than 20 nm. Accordingly, the decreases in the density of CuO and Al₂O₃ nanoparticles with diameters of 36 nm and 33 nm, respectively, were not significant since their size ranges were larger than 20 nm [87]. The experimental data from Eastman et al. [62] at room temperature is seen in Figure 1, where the enhancement of the nanofluid thermal conductivity of CuO was higher than Al₂O₃ by 28% at a 5% volume concentration. This enhancement return to a higher density of CuO (bulk density = 6.3 gm/cm³) than Al₂O₃ (bulk density = 3.9 gm/cm³) [47,85,86]. However, CuO and Al₂O₃ cannot be compared with the other two oxides (ZnO and SiO₂) because of their different diameters and the great dependence of the properties on the different preparation conditions. Comparisons should be done between nanofluids with the same base fluid, same particle size, and the same volume fraction. In this work, the thermal conductivity of CuO nanoparticles was higher than for Al₂O₃ nanoparticles, while their bulk thermal conductivity was close to each other (as seen in Table 1). However, the values of the intrinsic thermal conductivity of nanoparticles were due to their material type. The lower value of the nanoparticles' thermal conductivities compared to that of the bulk material can be explained as follows.

In experimental studies [90], the thermal conductivity of Si nanowires is less than the bulk value by an order of magnitude. In a molecular dynamics study [91], if the size of Si nanoparticles decreased below about 10 nm, their thermal conductivity decreased by two orders of magnitude compared to that of the bulk value. Mamand et al. [92,93] showed that the thermal conductivities of GaN and Ge nanowires are size-dependent. The reduction in value is due to both phonon confinement and boundary scattering effects; however, these depend on size-dependent parameters, such as the Debye temperature, surface roughness, the Gruneisen parameter, and the group velocity of phonons [94,95].

In NFs, the thermal energy interaction takes place at the nanoparticles' surface [52,63]. The specularity parameter, β , is a function of the surface roughness, μ [96], which reflects the probability of diffusive or specular scattering of phonons and is denoted by the following equation [55]: $\beta = 1 - 10\mu/D$, where D is the nanoparticles' diameter. The values of β are between 1 and 0. Due to the lack of experimental values for the surface roughness, β , was treated in this work as an adjustable parameter [93,94], where the values for all materials are listed in Table 2. These results suggested that nanoparticles' thermal conductivity through phonon scattering processes at the surface plays a significant role in transferring energy in NFs.

4.2. Liquid Nanolayer Thickness, h

The interface between the liquid and nanoparticles plays an important role that influences the thermal conductivity in NFs, which is known as the interface effect [97]. The liquid molecules form a layered structure close to the nanoparticle's surface [98]. This layer of atoms (nanolayer) around the particles is more ordered and its thermal conductivity is higher than that of the bulk liquid [56,99]. However, the nanolayer plays a key role in heat transfer but is not solely responsible for the thermal conductivity enhancement in NFs [32,100]. Recently, Song et al. [101] reported that the phonon frequency plays a vital role in the liquid and nanoparticles in NFs. An increase in the nanolayer molecule density and the ordered molecules causes an increase in the phonon group velocity and the phonon scattering at the particle–nanolayer interface will decrease. Thus, as the nanolayer thickness increases, the effective thermal conductivity will increase [83,97,102]. Many authors reported that the

nanolayer thickness, h , is in the range of 1–3 nm [56,63,64,72,99,100,103], while others have stated that a thickness of the nanolayer within the range of 1–3 nm does not affect the enhancement of the thermal conductivity in NFs [104]. Several authors [63,102] considered the nanolayers' thermal conductivity, K_{layer} , as being equal to $2K_m$ or even $3–5K_m$ with this range of thickness (1–3 nm) without getting a precise fitting to the experimental data at a wide range of particle volume concentrations.

In the present work, the effect of the nanolayer without the assumption of nanoparticle agglomeration was taken into account. To the best of our knowledge, the value of the nanolayer thickness, h , has unfortunately not been measured experimentally; therefore, it was used as an adjustable parameter (their values can be seen in Table 1), and according to Equation (6), the thermal conductivity ratio that provided the best fit to that of the experimental data was calculated.

5. A Brief Synopsis for Future Work

This trend in calculations is the first tendency toward finding nanoparticles' thermal conductivity (which is difficult practically) till now using the effective thermal conductivity data of NFs. The results can be used in other theoretical trends, such as statistically driven machine learning methods [18,19], for comparison. Moreover, this tendency can be used for finding the thermal conductivity of very small and large nanoparticles embedded in different kinds of fluids at different temperatures and comparing these results with experimental data.

Because of the different results found between the experimental data and theoretical models of the effective thermal conductivity of NFs in the literature, which shows contradictions, more work is needed to build a unified and universal theory for explaining the discrepancies and enhancement of the thermal conductivity of NFs.

6. Conclusions

This work concentrated on the utilization of theoretical trends for measuring nanoparticles' thermal conductivity, which is very difficult to achieve experimentally. The conclusions from this work are summarized in the following points:

- Prasher's model is a successful method for numerical calculations of the thermal conductivity of Al_2O_3 , CuO , ZnO , and SiO_2 nanoparticles suspended in water and EG base fluids.
- The nanoparticles' thermal conductivity is one of the main parameters that govern the thermal conductivity of NFs.
- The adjustable parameters, such as the specularity parameter, β , and the liquid nanolayer thickness, h , allowed for a correlation between the theoretical calculations and experimental data of NFs, indicating the significance of their effects and values.
- This trend of theoretical calculation is promising as a simple and easy method for finding the unknown thermal conductivity values of nanoparticles.

Funding: This research funded by Department of Physics, College of Science, university of Sulaimani.

Institutional Review Board Statement: This study did not involve humans or animals.

Informed Consent Statement: This study did not involve humans.

Data Availability Statement: All the data are referenced in the text.

Acknowledgments: The author would like to thank Shujadeen Baker and Mustafa Omar for their help in completing this work.

Conflicts of Interest: The authors declare no conflict of interest.

References

1. Duangthongsuk, W.; Wongwises, S. An experimental study on the heat transfer performance and pressure drop of TiO_2 -water nanofluids flowing under a turbulent flow regime. *Int. J. Heat Mass Transf.* **2010**, *53*, 334–344. [[CrossRef](#)]
2. Choi, S.U.S.; Eastman, J.A. Enhancing thermal conductivity of fluids with nanoparticles. *ASME Publ. Fed.* **1995**, *231*, 99–106.

3. Garg, J.; Poudel, B.; Chiesa, M.; Gordon, J.B.; Ma, J. Enhanced thermal conductivity and viscosity of copper nanoparticles in ethylene glycol nanofluid. *J. Appl. Phys.* **2008**, *103*, 074301–074306. [[CrossRef](#)]
4. Keblinski, P.; Prasher, R.; Eapen, J. Thermal conductance of nanofluids: Is the controversy over? *J. Nanopart. Res.* **2008**, *10*, 1089–1097. [[CrossRef](#)]
5. Wen, D.; Lin, G.; Vafaei, S.; Zhang, K. Review of nanofluids for heat transfer applications. *Particuology* **2009**, *7*, 141–150. [[CrossRef](#)]
6. Keblinski, P. Thermal conductivity of nanofluids. *Appl. Phys.* **2009**, *118*, 213–221.
7. Putra, N.; Roetzel, W.; Das, S.K. Natural convection of nano-fluids. *Heat Mass Transf.* **2003**, *39*, 775–784. [[CrossRef](#)]
8. Ghodsinezhad, H.; Sharifpur, M.J.; Meyer, P. Experimental investigation on cavity flow natural convection of Al₂O₃–water nanofluids. *Inter. Comm. Heat Mass Transfer.* **2016**, *76*, 316–324. [[CrossRef](#)]
9. Nkurikiyimfura, I.; Wang, Y.; Pan, Z. Heat transfer enhancement by magnetic nanofluids—A review. *Renew. Sustain. Energy Rev.* **2013**, *21*, 548–561. [[CrossRef](#)]
10. Tawfik, M.M. Experimental studies of nanofluid thermal conductivity enhancement and applications: A review. *Renew. Sustain. Energy Rev.* **2017**, *75*, 1239–1253. [[CrossRef](#)]
11. Gupta, M.; Singh, V.; Kumar, R.; Said, Z. A review on thermophysical properties of nanofluids and heat transfer applications. *Renew. Sustain. Energy Rev.* **2017**, *74*, 638–670. [[CrossRef](#)]
12. Nadooshan, A.A.; Eshgarf, H.; Afrand, M. Evaluating the effects of different parameters on rheological behavior of nanofluids: A comprehensive review. *Powder Technol.* **2018**, *338*, 342–353. [[CrossRef](#)]
13. Ali, H.M.; Babar, H.; Shah, T.R.; Sajid, M.U.; Qasim, M.A.; Javed, S. Preparation techniques of TiO₂ nanofluids and challenges: A review. *Appl. Sci.* **2018**, *8*, 587–617.
14. Sajid, M.U.; Ali, H.M. Recent advances in application of nanofluids in heat transfer devices: A critical review. *Renew. Sustain. Energy Rev.* **2019**, *103*, 556–592. [[CrossRef](#)]
15. Mahian, O.; Kianifar, A.; Kalogirou, S.A.; Pop, I.; Wongwises, S. A review of the applications of nanofluids in solar energy. *Int. J. Heat Mass Transf.* **2013**, *57*, 582–594. [[CrossRef](#)]
16. Babar, H.; Sajid, M.; Ali, H. Viscosity of hybrid nanofluids: A critical review. *Science* **2019**, *23*, 1713–1754. [[CrossRef](#)]
17. Izadi, S.; Armaghani, T.; Ghasemiasl, R.; Chamkha, A.J.; Molana, M. A comprehensive review on mixed convection of nanofluids in various shapes of enclosures. *Powder Technol.* **2019**, *343*, 880–907. [[CrossRef](#)]
18. Zhang, Y.; Xu, X. Predicting the thermal conductivity enhancement of nanofluids using computational intelligence. *Phys. Lett. A* **2020**, *384*, 126500. [[CrossRef](#)]
19. Maleki, A.; Haghighi, A.; Mahariq, I. Machine learning-based approaches for modeling thermophysical properties of hybrid nanofluids: A comprehensive review. *J. Mol. Liq.* **2021**, *322*, 114843. [[CrossRef](#)]
20. Asadi, A.; Aberoumand, S.; Moradikazerouni, A.; Pourfattah, F.; Żyła, G.; Estellé, P.; Mahian, O.; Wongwises, S.; Nguyen, H.M.; Arabkoohsar, A. Recent advances in preparation methods and thermophysical properties of oil-based nanofluids: A state-of-the-art review. *Powder Technol.* **2019**, *352*, 209–226. [[CrossRef](#)]
21. Xue, Q.Z. Model for Effective Thermal Conductivity of Nanofluids. *Phys. Lett. A* **2003**, *307*, 313–317. [[CrossRef](#)]
22. Wang, B.X.; Zhou, L.P.; Peng, X.F. A Fractal Model for Predicting the Effective Thermal Conductivity of Liquid with Suspension of Nanoparticles. *Int. J. Heat Mass Transfer.* **2003**, *46*, 2665–2672. [[CrossRef](#)]
23. Jang, S.P.; Choi, S.U.S. Role of Brownian Motion in the Enhanced Thermal Conductivity of Nanofluids. *Appl. Phys. Lett.* **2004**, *84*, 4316–4318. [[CrossRef](#)]
24. Koo, J.; Kleinstreuer, C. A New Thermal Conductivity Model for Nanofluids. *J. Nanopart. Res.* **2004**, *6*, 577–588. [[CrossRef](#)]
25. Bhattacharya, P.; Saha, S.K.; Yadav, A.; Phelan, P.E.; Prasher, R.S. Brownian Dynamics Simulation to Determine the Effective Thermal Conductivity of Nanofluids. *J. Appl. Phys.* **2004**, *95*, 6492–6494. [[CrossRef](#)]
26. Xuan, Y.; Li, Q.; Hu, W. Aggregation structure and thermal conductivity of nanofluids. *J. AIChE* **2003**, *49*, 1038–1043. [[CrossRef](#)]
27. Kumar, D.H.; Patel, H.E.; Ragev Kumar, V.R.; Sundararajan, T.; Pradeep, T.; Das, S.K. Model for heat conduction in nanofluids. *Phys. Rev. Lett.* **2004**, *93*, 144301–144304. [[CrossRef](#)]
28. Prasher, R.; Bhattacharya, P.; Phelan, P.E. Thermal conductivity of nanoscale colloidal solutions (nanofluids). *Phys. Rev. Lett.* **2005**, *94*, 025901–025904. [[CrossRef](#)]
29. Prasher, R.; Phelan, P.E.; Bhattacharya, P. Effect of aggregation kinetics on the thermal conductivity of nanoscale colloidal solutions (nanofluids). *Nano Lett.* **2006**, *6*, 1529. [[CrossRef](#)]
30. Patel, H.E.; Sundararajan, T.; Das, S.K. A cell model approach for thermal conductivity of nanofluids. *J. Nanopart. Res.* **2008**, *10*, 87–97. [[CrossRef](#)]
31. Kihm, K.D.; Chon, C.H.; Lee, J.S.; Choi, S.U.S. A new heat propagation velocity prevails over Brownian particle velocities in determining the thermal conductivities of nanofluids. *Nanoscale Res. Lett.* **2011**, *6*, 361–369. [[CrossRef](#)]
32. Karthikeyan, N.R.; Philip, J.; Raj, B. Effect of clustering on the thermal conductivity of Nanofluids. *Mater. Chem. Phys.* **2008**, *109*, 50–55. [[CrossRef](#)]
33. Jang, S.P.; Choi, S.U.S. Effect of various parameters on nanofluid thermal conductivity. *J. Heat Transf.* **2007**, *129*, 617–623. [[CrossRef](#)]
34. Evans, W.; Fish, J.; Keblinski, P. Role of Brownian motion hydrodynamics on nanofluid thermal conductivity. *Appl. Phys. Lett.* **2006**, *88*, 093116–093118. [[CrossRef](#)]
35. Chon, C.H.; Kihm, K.D.; Lee, S.P.; Choi, S.U.S. Empirical correlation finding the role of temperature and particle size for nanofluid (Al₂O₃) thermal conductivity enhancement. *Appl. Phys. Lett.* **2005**, *87*, 153107–153109. [[CrossRef](#)]

36. Mintsas, H.A.; Roy, G.; Nguyen, C.T.; Doucet, D. New temperature dependent thermal conductivity data for water-based nanofluids. *Int. J. Therm. Sci.* **2009**, *48*, 363–371. [[CrossRef](#)]
37. Hong, J.; Kim, S.H.; Kim, D. Effect of laser irradiation on thermal conductivity of ZnO nanofluids. *J. Phys. Conf. Ser.* **2007**, *59*, 301–304. [[CrossRef](#)]
38. He, Y.; Jin, Y.; Chen, H.; Ding, Y.; Cang, D.; Lu, H. Heat transfer and flow behavior of aqueous suspensions of TiO₂ nanoparticles (nanofluids) flowing upward through a vertical pipe. *Int. J. Heat Mass Transf.* **2007**, *50*, 2272–2281. [[CrossRef](#)]
39. Sundar, L.S.; Sharma, K.V. Thermal conductivity enhancement of nanoparticles in distilled water. *Int. J. Nanoparticles* **2008**, *1*, 66–77. [[CrossRef](#)]
40. Kim, S.H.; Choi, S.R.; Kim, D. Thermal conductivity of metal-oxide nanofluids: Particle size dependence and effect of laser irradiation. *ASME J. Heat Transf.* **2007**, *129*, 298–307. [[CrossRef](#)]
41. Chen, G.; Yu, W.; Singh, D.; Cookson, D.; Routbort, J. Application of SAXS to the study of particle size dependent thermal conductivity in silica nanofluids. *J. Nanopart. Res.* **2008**, *10*, 1109–1114. [[CrossRef](#)]
42. Beck, M.P.; Yuan, Y.; Warriar, P.; Teja, A.S. The effect of particle size on the thermal conductivity of alumina nanofluids. *J. Nanopart. Res.* **2009**, *11*, 1129–1136. [[CrossRef](#)]
43. Timofeeva, E.V.; Yu, W.; France, D.M.; Singh, D.; Routbort, J.L. Base fluid and temperature effects on the heat transfer characteristics of SiC in ethylene glycol/H₂O and H₂O nanofluids. *J. Appl. Phys.* **2011**, *109*, 014914–014918. [[CrossRef](#)]
44. Timofeeva, E.V.; Smith, D.S.; Yu, W.; France, D.M.; Singh, D.; Routbort, J.L. Particle size and interfacial effects on thermo-physical and heat transfer characteristics of water-based a-SiC nanofluids. *Nanotechnology* **2010**, *21*, 215703–215713. [[CrossRef](#)] [[PubMed](#)]
45. Darvanjooghi, M.H.K.; Esfahany, M.N. Experimental investigation of the effect of nanoparticle size on thermal conductivity of in-situ prepared silica–ethanol nanofluid. *Int. Com. Heat Mass Transf.* **2016**, *77*, 148–154. [[CrossRef](#)]
46. Yu, W.; France, D.M.; Routbort, J.L.; Choi, S.U.S. Review and Comparison of Nanofluid Thermal Conductivity and Heat Transfer Enhancements. *Heat Transf. Eng.* **2008**, *29*, 432–460. [[CrossRef](#)]
47. Pryazhnikov, M.I.; Minakov, A.V.; Rudyak, V.Y.; Guzei, D.V. Thermal conductivity measurements of nanofluids. *Int. J. Heat Mass Transf.* **2017**, *104*, 1275–1282. [[CrossRef](#)]
48. Ceotto, D.; Rudyak, V.Y. Phenomenological Formula for Thermal Conductivity Coefficient of Water Based Nanofluids. *Colloid J.* **2016**, *78*, 509–514. [[CrossRef](#)]
49. Zhua, H.; Zhang, C.; Liu, S.; Tang, Y.; Yina, Y. Effects of nanoparticle clustering and alignment on thermal conductivities of Fe₃O₄ aqueous nanofluids. *Appl. Phys. Lett.* **2006**, *89*, 023123–023125. [[CrossRef](#)]
50. Aybar, H.Ş.; Sharifpur, M.; Azizian, M.R.; Mehrabi, M.; Meyer, J.P. A Review of Thermal Conductivity Models for Nanofluids. *Heat Transf. Eng.* **2015**, *36*, 1085–1171. [[CrossRef](#)]
51. Calvin, H.L.; Peterson, G.P. Experimental investigation of temperature and volume fraction variations on the effective thermal conductivity of nanoparticle suspensions (nanofluids). *J. Appl. Phys.* **2006**, *99*, 084314–084322.
52. Yu, W.; Xie, H.; Chen, L.; Li, Y. Investigation of thermal conductivity and viscosity of ethylene glycol based ZnO nanofluid. *Thermochim. Acta* **2009**, *491*, 92–96.
53. Ho, C.J.; Liu, W.K.; Chang, Y.S.; Lin, C.C. Natural convection heat transfer of alumina-water nanofluid in vertical square enclosures: An experimental study. *Int. J. Therm. Sci.* **2010**, *49*, 1345–1353. [[CrossRef](#)]
54. Prasher, R. Thermal conductivity of composite of aligned nanoscale and microscale wires and pores. *J. Appl. Phys.* **2006**, *100*, 034307–034317. [[CrossRef](#)]
55. Liang, L.H.; Li, B. Size-dependent thermal conductivity of nanoscale semiconducting systems. *Phys. Rev. B* **2006**, *73*, 153303–153306. [[CrossRef](#)]
56. Yu, W.; Choi, S.U.S. The role of interfacial layers in the enhanced thermal conductivity of nanofluids: A renovated Maxwell model. *J. Nanoparticle Res.* **2003**, *5*, 167–171. [[CrossRef](#)]
57. Gao, T.; Jelle, B.P. Thermal conductivity of TiO₂ nanotubes. *J. Phys. Chem. C* **2013**, *117*, 1401. [[CrossRef](#)]
58. Teja, A.S.; Beck, M.P.; Yuan, Y.; Warriar, P. The limiting behavior of the thermal conductivity of nanoparticles and nanofluids. *J. Appl. Phys.* **2010**, *107*, 114319–114322. [[CrossRef](#)]
59. Gao, T.; Jelle, B.P. Thermal conductivity of amorphous silica nanoparticles. *J. Nanoparticle Res.* **2019**, *21*, 108–113. [[CrossRef](#)]
60. Yu, C.-J.; Richter, A.G.; Datta, A.; Durbin, M.K.; Dutta, P. Observation of molecular layering in thin liquid films using X-ray reflectivity. *Phys. Rev. Lett.* **1999**, *82*, 2326–2330. [[CrossRef](#)]
61. Maxwell, J.C. *Electricity and Magnetism*; Clarendon Press: Oxford, UK, 1873.
62. Eastman, J.A.; Choi, U.S.; Li, S.; Thompson, L.J.; Lee, S. Enhanced thermal conductivity through the development of nanofluids. *Mat. Res. Soc. Symp. Proc.* **1997**, *457*, 01997–019105. [[CrossRef](#)]
63. Kole, M.; Dey, T.K. Role of interfacial layer and clustering on the effective thermal conductivity of CuO–gear oil nanofluids. *Exp. Therm. Fluid Sci.* **2011**, *35*, 1490–1495. [[CrossRef](#)]
64. Feng, Y.; Yu, B.; Xu, P.; Zou, M. The effective thermal conductivity of nanofluids based on the nanolayer and the aggregation of nanoparticles. *J. Phys. D Appl. Phys.* **2007**, *40*, 3164–3171. [[CrossRef](#)]
65. Huang, Z.X.; Tang, Z.; Yu, J.; Bai, S. Thermal conductivity of nanoscale polycrystalline ZnO thin films. *Physica B* **2011**, *406*, 818–823. [[CrossRef](#)]
66. Olorunyolemi, T.; Birnboim, A.; Carmel, Y.; Wilson, O.; Lloyd, I. Thermal Conductivity of Zinc Oxide: From Green to Sintered State. *J. Am. Ceram. Soc.* **2002**, *85*, 1249–1253. [[CrossRef](#)]

67. Chen, H.; Ding, Y.; He, Y.; Tan, C. Rheological behaviour of ethylene glycol based titania nanofluids. *Chem. Phys. Lett.* **2007**, *444*, 333–337. [[CrossRef](#)]
68. Geiger, G.H.; Poirier, D.R. *Transport Phenomena in Metallurgy*, 19; Addison-Wesley: Boston, MA, USA, 1973; p. 190.
69. Kisi, E.; Ekombe, M.M. Parameters for the wurtzite structure of ZnS and ZnO using powder neutron diffraction. *Acta Crystallographica Sect. C* **1989**, *45*, 1867–1870. [[CrossRef](#)]
70. Kang, H.U.; Kim, S.H.; Oh, J.M. Estimation of Thermal Conductivity of Nanofluid Using Experimental Effective Particle Volume. *Exp. Heat Transfer*. **2006**, *19*, 181–191. [[CrossRef](#)]
71. Chen, G. Nonlocal and Nonequilibrium Heat Conduction in the Vicinity of Nanoparticles. *J. Heat Transf.* **1996**, *118*, 539–545. [[CrossRef](#)]
72. Senthilraja, S.; Vijayakumar, K.; Gangadevi, R. A comparative study on thermal conductivity of Al₂O₃/water, CuO/water and Al₂O₃-CuO/water nanofluids. *Dig. J. Nanomat. Biol.* **2015**, *10*, 1449–1458.
73. Haynes, W.M. *CRC Handbook of Chemistry and Physics*, 92nd ed.; CRC Press: Boca Raton, FL, USA, 2011; ISBN 978-1439855119.
74. Seetawan, U.; Jugsujinda, S.; Seetawan, T.; Ratchasin, A.; Euvananont, C.; Junin, C.; Thanachayanont, C.; Chainaronk, P. Effect of Calcinations Temperature on Crystallography and Nanoparticles in ZnO Disk. *Mat. Sci. Appl.* **2011**, *2*, 1302–1306. [[CrossRef](#)]
75. Richet, P.; Bottinga, Y.; Denielou, L.; Petitet, J.P.; Tequi, C. Thermodynamic properties of quartz, cristobalite and amorphous SiO₂: Drop calorimetry measurements between 1000 and 1800 K and a review from 0 to 2000 K. *Geochim. Acta* **1982**, *46*, 2639–2658. [[CrossRef](#)]
76. Brown, I.D.; Shannon, R.D. Empirical bond-strength-bond length curves for oxides. *Acta Crystallography A* **1973**, *29*, 266–283. [[CrossRef](#)]
77. Vinodkumar, T.; Reddy, B.M. *Catalytic Combustion over Cheaper Metal Oxides*; Nova Science Publishers: Hauppauge, NY, USA, 2011; ISBN 978-1-61324-279-7.
78. Zumdahl, S.S. *Chemical Principles*, 6th ed.; Houghton Mifflin Company: Boston, MA, USA, 2009; ISBN 978-0-618-94690-7.
79. Gutierrez, G.; Johansson, B. Molecular dynamics study of structural properties of amorphous Al₂O₃. *Phys. Rev. B* **2002**, *65*, 104202–104210. [[CrossRef](#)]
80. Ahmed, A.; Elvati, P.; Violi, A. Size- and phase-dependent structure of copper (II) oxidenanostructures. *RSC Adv.* **2015**, *5*, 35033–35054. [[CrossRef](#)]
81. Chase, M.W. Thermochemical Tables, Fourth Edition. *J. Phys. Chem. Ref. Data Monogr.* **1998**, *9*, 1–195.
82. Polak, M.L.; Gilles, M.K.; Ho, J.; Lineberger, W.C. Photoelectron spectroscopy of copper oxide (CuO-). *J. Phys. Chem.* **1991**, *95*, 3460–3463. [[CrossRef](#)]
83. Chase, M.W., Jr. *NIST-JANAF Thermochemical Tables*, 4th ed.; American Institute of Physics: College Park, MD, USA, 1998.
84. Xie, H.; Yu, W.; Chen, W. MgO nanofluids: Higher thermal conductivity and lower viscosity among ethylene glycol-based nanofluids containing oxide nanoparticles. *J. Exp. Nanosci.* **2010**, *5*, 463–472. [[CrossRef](#)]
85. Rudyak, V.Y.; Belkin, A.A. Simulation of transport coefficients, Nanosystems. *Phys. Chem. Math.* **2010**, *1*, 156–177.
86. Rudyak, V.Y.; Belkin, A.A.; Tomilina, E.A. On the thermal conductivity of nanofluids. *Tech. Phys. Lett.* **2010**, *36*, 49–54. [[CrossRef](#)]
87. Abdullah, B.J.; Omar, M.S.; Jiang, Q. Size dependence of the bulk modulus of Si nanocrystals. *Sādhanā* **2018**, *43*, 174–179. [[CrossRef](#)]
88. Siegel, J.; Lyutakov, O.; Rybka, V.; Kolska, Z.; Švorčík, V. Properties of gold nanostructures sputtered on glass. *Nanoscale Res. Lett.* **2011**, *6*, 96–104. [[CrossRef](#)]
89. Opalinska, A.; Malka, I.; Dzwolowak, W.; Chudoba, T.; Presz, A.; Lojkowski, W. Size-dependent density of zirconia nanoparticles. *Beilstein J. Nanotechnol.* **2015**, *6*, 27–35. [[CrossRef](#)] [[PubMed](#)]
90. Li, D.; Wu, Y.; Kim, P.; Shi, L.; Yang, P.; Majumdar, A. Thermal conductivity of individual silicon nanowires. *J. Appl. Phys. Lett.* **2003**, *83*, 2934–2936. [[CrossRef](#)]
91. Fang, K.C.; Weng, C.L.; Ju, S.P. An investigation into the structural features and thermal conductivity of silicon nanoparticles using molecular dynamics simulations. *Nanotechnology* **2006**, *17*, 3909–3914. [[CrossRef](#)]
92. Mamand, S.M.; Omar, M.S.; Muhammad, A.J. Nanoscale size dependence parameters on lattice thermal conductivity of Wurtzite GaN nanowires. *Mater. Res. Bull.* **2012**, *47*, 1264–1272. [[CrossRef](#)]
93. Mamand, S.M.; Omar, M.S. Effect of Parameters on Lattice Thermal Conductivity in Germanium Nanowires. *Adv. Mater. Res.* **2014**, *832*, 33–38. [[CrossRef](#)]
94. Park, Y.H.; Kim, J.; Kim, H.; Kim, I.; Lee, K.-Y.; Seo, D.; Choi, H.; Kim, W. Thermal conductivity of VLS-grown rough Si nanowires with various surface roughnesses and diameters. *Appl. Phys. A* **2011**, *104*, 7–14. [[CrossRef](#)]
95. Zou, J.; Balandin, A. Phonon heat conduction in a semiconductor nanowire. *J. Appl. Phys.* **2001**, *89*, 2932–2938. [[CrossRef](#)]
96. Ziman, J.M. *Electrons and Phonons*; Clarendon: Oxford, UK, 1960.
97. Xie, H.Q.; Fujii, M.; Zhang, X. Effect of interfacial nanolayer on the effective thermal conductivity of nanoparticle–fluid mixture. *Int. J. Heat Mass Transf.* **2005**, *48*, 2926–2932. [[CrossRef](#)]
98. Henderson, J.R.; Swol, F. On the interface between a fluid and a planar wall: Theory and simulations of a hard sphere fluid at a hard wall. *Mol. Phys.* **1984**, *51*, 991–1010. [[CrossRef](#)]
99. Yu, C.J.; Richter, A.G.; Datta, A.; Durbin, M.K.; Dutta, P. Molecular layering in a liquid on a solid substrate: An X-ray reflectivity study. *Physica B* **2000**, *283*, 27–31. [[CrossRef](#)]

100. Yu, W.; Choi, S.U.S. The role of interfacial layers in the enhanced thermal conductivity of nanofluids: A renovated Hamilton-Crosser. *J. Nanoparticle Res.* **2004**, *6*, 355–361. [[CrossRef](#)]
101. Song, D.; Jing, D.; Ma, W.; Zhang, X. High thermal conductivity of nanoparticles not necessarily contributing more to nanofluids. *Appl. Phys. Lett.* **2018**, *113*, 223104–223109. [[CrossRef](#)]
102. Leong, K.C.; Yang, C.; Murshed, S.M.S. A model for the thermal conductivity of nanofluids—the effect of interfacial layer. *J. Nanopart. Res.* **2006**, *8*, 245–254. [[CrossRef](#)]
103. Keblinski, P.; Phillpot, S.; Choi, S.U.S.; Eastman, J.A. Mechanisms of heat flow in suspensions of nano-sized particles (nanofluids). *Inter. J. Heat Mass Transf.* **2002**, *45*, 855–863. [[CrossRef](#)]
104. Murshed, S.M.S.; Leong, K.C.; Yang, C. A combined model for the effective thermal conductivity of nanofluids. *Appl. Therm. Eng.* **2009**, *29*, 2477–2483. [[CrossRef](#)]